THE JOURNAL OF PHYSICAL CHEMISTRY C

Article

pubs.acs.org/JPCC

Observation of Mediated Cascade Energy Transfer in Europium-Doped ZnO Nanowalls by 1,10-Phenanthroline

Jung-Soo Kang,[†] Yong-Kwang Jeong,[‡] Jun-Gill Kang,[‡] Liyan Zhao,[†] Youngku Sohn,[†,§] Debabrata Pradhan,[†,⊥] and K. T. Leung*[,†]

[†]WATLab and Department of Chemistry, University of Waterloo, Waterloo, Ontario N2L 3G1, Canada

[‡]Department of Chemistry, Chungnam National University, Daejeon, 305-764, Republic of Korea

Supporting Information

ABSTRACT: Embedding rare earth ions into a host material such as alkali halides, semiconductors, and metal oxides has been extensively studied, with the goal to improve performance in light emitting devices and biomedicine. Here, Europium-embedded ZnO nanowall structures have been achieved by a facile electrochemical deposition method. Upon Eu embedment, the nanowalls were found to become thicker and stacked. X-ray photoemission study revealed that $Zn(OH)_2$ was more dominant than ZnO near the surface and it confirmed that Eu(III) was uniformly distributed in the $ZnO-Zn(OH)_2$ core−shell structure. We also measured the photoluminescence spectra of as-grown, heat-treated and 1,10-phenanthroline surface-functionalized ZnO nanowalls samples, which led us to propose a unique cascade energy transfer model between ZnO, 1,10-phenanthroline, and Eu^{3+} ion.

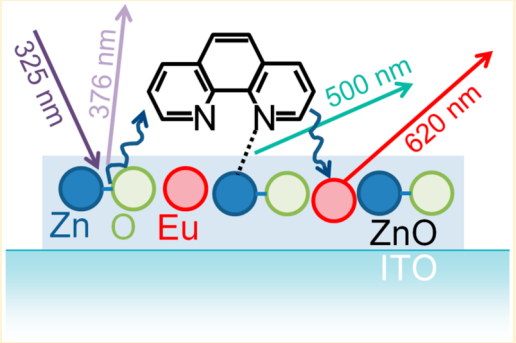

INTRODUCTION

Rare earth doped ZnO nanomaterials are recognized as promising candidates for applications in optoelectronic and light-emitting devices, spintronics and photocatalysis.[1−10] Among rare earth ions, the trivalent Eu^{3+} ion has attracted great interest because of its unique optical properties, arisen from the hypersensitive $^5D_0 \rightarrow {}^7F_2$ red emission (~620 nm) from Eu(III).[11−13] Recently, nanostructured Eu-doped ZnO has been prepared by various methods, including hydrothermal synthesis, thermal evaporation, electrochemical deposition, sol−gel, and laser ablation.[14−26] These techniques produced Eu-doped ZnO nanostructures with various morphologies including nanospheres, nanoparticles, nanoneedles, nanorods, nanowires and nanoflowers.[20−25] Upon excitation by UV irradiation, these $ZnO:Eu^{3+}$ nanomaterials produced a band-edge emission at 369 nm, a broad defect-emission at 500−750 nm and/or a red emission from Eu^{3+}. The appearance of the red emission was dependent on the excitation energy and on whether thermal annealing has been performed or not. The Eu^{3+}-related luminescence arisen from the band gap excitation has been discussed in terms of the energy transfer from ZnO to Eu^{3+}.[8,24,26] Alternatively, the red emission from $ZnO:Eu^{3+}$ nanospheres and nanorods could also be attributed to the direct excitation of Eu^{3+} to a charge-transfer state, instead of the energy transfer pathway.[25]

Detailed knowledge of the structural and optical properties of $ZnO:Eu^{3+}$ nanostructured materials grown on a selected substrate is important to industrial applications. Extensive research has been conducted to deposit ZnO films or nanostructures on a transparent substrate like indium tin oxide coated glass (ITO-glass), and to characterize their structural, optical and electrical properties.[27−35] The deep-level emission from ZnO, appearing in the visible region, has been found to be highly dependent on its morphology, defects and doping.[35−41] Here, we fabricate ZnO nanowalls doped with various concentrations of Eu^{3+} on ITO-glass by a simple electrochemical deposition method and investigate the photophysical properties of the prepared nanowalls on ITO-glass. We also clarify the change in the chemical-state composition of Eu by depth-profiling X-ray photoelectron spectroscopy (XPS). Furthermore, by functionalizing the surface of $ZnO:Eu^{3+}$ nanowalls using an ultraviolet range energy donor such as 1,10-phenanthroline (phen), we investigate its effect on the photoluminescence (PL) of the Eu-doped ZnO nanowalls. We propose a cascade energy transfer model from ZnO to Eu^{3+} via phen, in order to provide new insight into the emission and energy transfer processes in surface-functionalized $ZnO:Eu^{3+}$ nanostructures.

RESULTS AND DISCUSSION

Figure 1 shows the SEM images of undoped and Eu-doped ZnO nanowalls. For the undoped ZnO sample, the ledge thickness of the pristine nanowalls is measured to be 50−100 nm (Figure 1a). On the other hand, Eu-embedded ZnO nanowalls are found to be stacked together, forming relatively thicker structures with the ledge thickness of 150−400 nm for

Received: September 8, 2014
Revised: January 2, 2015
Published: January 2, 2015

DOI: 10.1021/jp5090795
J. Phys. Chem. C 2015, 119, 2142−2147

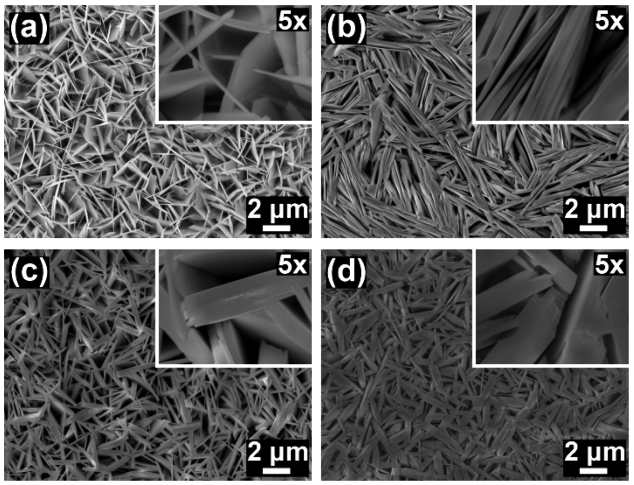

Figure 1. SEM images of ZnO nanowalls deposited at 70 °C on ITO-glass in (a) 0.10 M $Zn(NO_3)_2{\cdot}6H_2O$ mixed with 0.10 M KCl, and with additional (b) 0.01 M, (c) 0.05 M, and (d) 0.10 M $Eu(NO_3)_3{\cdot}5H_2O$.

0.01 M Eu-doped nanowalls (Figure 1b) and 300−700 nm for 0.05 M (Figure 1c) and 0.10 M Eu-doped nanowalls (Figure 1d). Although the stacking of individual nanowalls in Eu-embedded samples is quite apparent in the nanowalls with less dopant, heavier doped nanowalls appear merged together forming a thicker edge with smoother surface.

Figure 2 shows the XPS spectra, collected as a function of sputtering depth, of the Eu 3d, Zn 2p, and O 1s regions of Eu-doped ZnO nanowalls obtained in the 0.05:0.1 M Eu^{3+}:Zn^{2+} electrolyte. For the as-prepared sample, a single broad O 1s peak at 532.9 eV is observed. With increasing Ar^+ ion sputtering time, a new peak emerges at 531.2 eV and becomes more dominant. The O 1s peaks at 532.9 and 531.2 eV can be attributed to $Zn(OH)_2$ and/or Eu hydroxides and to ZnO, respectively. The Zn $2p_{3/2}$ (Zn $2p_{1/2}$) peak, initially located at 1023.3 eV (1046.4 eV) before sputtering, is found to evolve into a considerably more intense peak at 1022.5 eV (1045.6 eV) upon sputtering for 500 s. We also observe a strong Eu(III) Eu $3d_{5/2}$ (Eu $3d_{3/2}$) peak at 1135.5 eV (1165.0 eV) and a considerably weaker Eu(II) Eu $3d_{5/2}$ (Eu $3d_{3/2}$) feature at 1126.5 eV (1156 eV).[42] This indicates that both Eu(III) and Eu(II) coexist in the ZnO nanowall structure. The relative Eu(III)/Eu(II) composition ratio is 1.8 and found to be nearly constant with increasing sputtering depth. Of special interest is the definite presence of Eu(II) even though only Eu(III) ions were used in our electrolytes. Because of the larger ionic radius of Eu(III) than that of Zn(II) and of the charge imbalance, it is less likely for Eu(III) than Eu(II) to be uniformly incorporated into ZnO matrix. It therefore appears that Eu(III) is first reduced to Eu(II) in order to alleviate the charge imbalance, thereby creating defects inside the nanowalls, during the electrodeposition.

For pristine ZnO nanowalls, Pradhan et al. demonstrated their $ZnO/Zn(OH)_2$ core/shell structure, along with details of the growth mechanism consistent with the XPS results of electrodeposited ZnO nanostructures.[43,44] The observed O 1s and Zn 2p spectra for the Eu-doped ZnO nanowalls closely resemble those for undoped ZnO nanowalls reported by Pradhan et al., indicating a similar $ZnO/Zn(OH)_2$ core/shell structure that is likely obtained by a similar growth mechanism.

The PL spectra of the ZnO nanowalls grown on ITO-glass from various concentrations of Eu^{3+} were also measured at

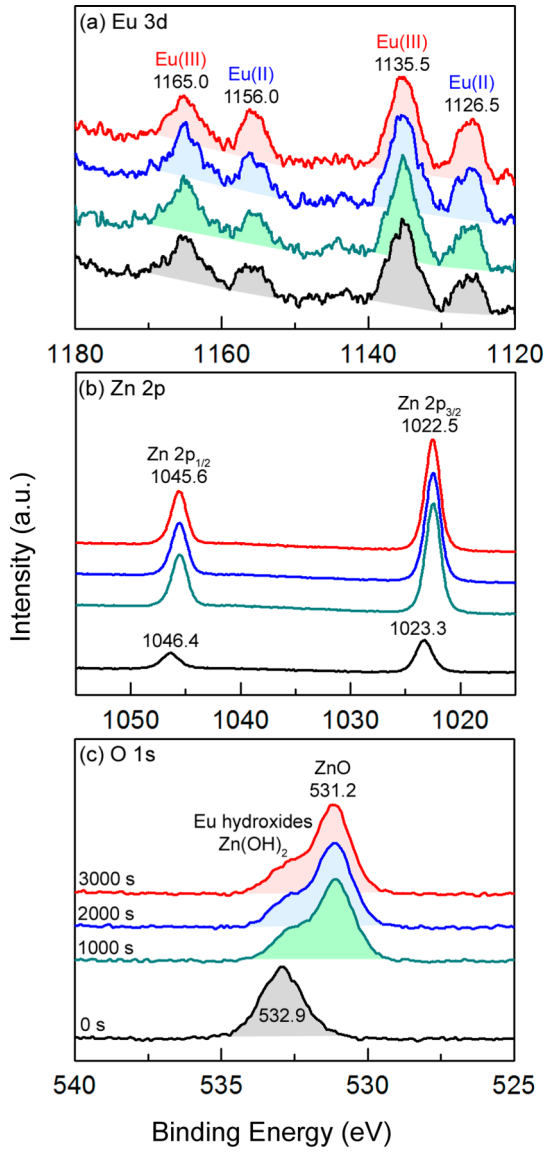

Figure 2. XPS spectra of (a) Eu 3d, (b) Zn 2p, and (c) O 1s regions of as-deposited Eu-embedded ZnO nanowalls before sputtering and with a total sputtering time of 1000, 2000, and 3000 s.

room temperature. As shown in Figure 3, the spectral shape of the ZnO:Eu^{3+} nanowalls is almost independent of the Eu^{3+} concentration, i.e., there is virtually no difference in the spectral shapes between the undoped and the doped nanowall structures. Upon excitation by a He−Cd 325 nm line, both the undoped and doped nanowalls exhibit only one broad band in the 400−700 nm region. The visible emission from ZnO generally originates from various intrinsic defects. For example, the green emission can be attributed to neutral and ionized oxygen vacancies, while the orange-red emission is associated with neutral and charged zinc interstitials or oxygen interstitial.[36,39] Alternatively, the green and yellow emissions from ZnO could also correspond to the presence of OH^- and $Zn(OH)_2$ on the surface, respectively.[40,41] The excitation spectrum of the deep-level emission illustrated in Figure 3a shows that the origin of the broad visible emission is the ZnO host and it confirms the electronic transitions from the valence band to the upper conduction band. The band-edge emission peak at 370 nm is therefore not likely to be produced by the as-

DOI: 10.1021/jp5090795
J. Phys. Chem. C 2015, 119, 2142−2147

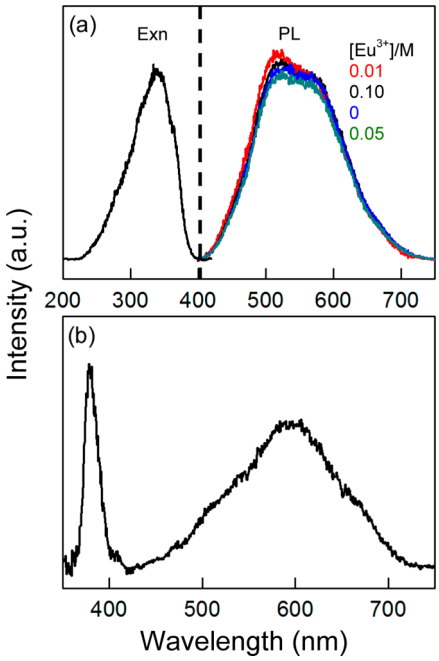

Figure 3. (a) PL (with $\lambda_{excitation}$ = 325 nm) and excitation (exn) (with $\lambda_{emission}$ = 590 nm) spectra of ZnO:Eu^{3+} nanowalls for various Eu^{3+} concentrations and (b) PL (with $\lambda_{excitation}$ = 325 nm) spectrum of thermally treated ZnO:Eu^{3+}.

prepared undoped and doped nanowalls upon excitation at 325 nm. These results indicate that for the nanowall structures on ITO-glass, the radiative transition from the conduction band is suppressed by the energy transfer to the upper states of the intrinsic defects. Furthermore, the sharp Eu^{3+} lines at 620 nm are not observed from the ZnO:Eu^{3+} nanowalls on ITO-glass. These results are very similar to those of ZnO:Eu^{3+} films grown by solution chemistry.[26]

The formation of ionized vacancies and OH^- on the surface of the nanowalls from the aqueous solution is clearly seen from the XPS results (Figure 2). The red emission from Eu^{3+} would eventually be quenched by these defects. To investigate the effects of reducing the defects, we annealed the as-prepared nanowalls on ITO-glass at 300 °C for 1 h under oxygen flow. SEM study indicates that the morphology of the postannealed nanowalls on ITO-glass was not changed by the heat treatment (not shown). As shown in Figure 3b, the 325 nm excitation produces not only the deep-level emission band but also a strong, sharp band-edge emission band at 378 nm. Annealing also reduces the intensity of the deep-level emission by more than half, with the green emission being quenched more than the orange-red emission, which shifts the band maximum to 600 nm. This spectral change indicates that more OH^--related defects and the oxygen-related vacancies are removed than other intrinsic defects by thermal annealing. However, the sharp 620 nm line characteristic of Eu^{3+} remains absent, which suggests that the energy transfer from the ZnO host to the doped Eu^{3+} ion does not occur efficiently.

As shown in XPS analysis, Eu^{3+} ions are also present at the surface layer, we attempted to induce the red emission from Eu^{3+} by modifying the ZnO:Eu^{3+} nanowall surface with phen. For a Eu^{3+} complex with phen, the sensitized emission from Eu^{3+} can be effectively generated by phen.[45,46] First, the surfaces of the as-grown and the postannealed ZnO:Eu^{3+} nanowalls were modified by dipping them in phen with three different concentrations (0.010, 0.050, and 0.10 M) in CH_2Cl_2 for 30 s then PL with excitation wavelength of 325 nm were measured. Evidently, surface-functionalization with 0.010 M solution of phen has no effect on the PL spectrum for the as-grown ZnO:Eu^{3+} nanowalls (Figure 4a). In contrast, the same

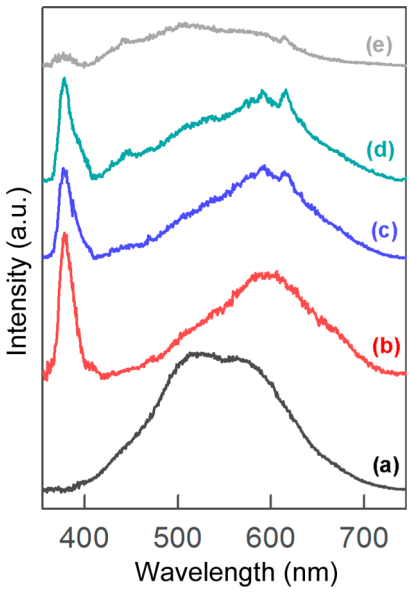

Figure 4. PL (with $\lambda_{excitation}$ = 325 nm) emission spectra of (a) as-grown ZnO:Eu^{3+} nanowalls sample surface-functionalized with 0.010 M phen, and annealed samples surface-functionalized (b) without and with (c) 0.010 M, (d) 0.050 M, and (e) 0.10 M of phen.

treatment for the postannealed ZnO:Eu^{3+} nanowalls results in a sharp red emission band from Eu^{3+} at 620 nm, as shown in Figure 4c. Except for the emergence of this sharp 620 nm red emission and the slight intensity reduction for the band-edge emission at 376 nm, the spectral shape of the phen-treated nanowalls (Figure 4c) is almost the same as the postannealed nanowalls without the phen treatment (Figure 4b). The appearance of the 620 nm peak indicates that the Eu^{3+} ions on the surface layer are coordinated to phen, and the coordinated phen molecules trigger energy transfer process to Eu^{3+} ions which produce the red emission. When treated with a higher phen concentration of 0.050 M (Figure 4d), the blue-green emission becomes discernibly more intense. For treatment with an even higher phen concentration of 0.10 M (Figure 4e), spectral intensity above 480 nm has been significantly reduced relative to that functionalized with 0.05 M phen, with the blue-green emission becoming stronger than the 600 nm emission. The band-edge emission at 376 nm has also been quenched significantly. For comparison, PL and excitation spectra of an Eu–phen complex, $[Eu(phen)_2]\cdot(NO_3)_3$, have also been obtained (Supporting Information, Figure S1), which shows that its excitation spectrum does not match with the excitation spectrum of the Eu-doped ZnO nanowalls shown in Figure 3a.

To investigate the energy transfer path and the origin of blue-green emission enhancement, we also modified the surface of the annealed nanowalls by ethylenediamine (en), which has two nitrogen atoms like phen. En acts as a bidentate ligand to form a complex with Eu^{3+}, but en is nonluminescent. Figure 5 shows the PL emission spectra of the postannealed ZnO:Eu^{3+} nanowalls on ITO-glass without and with en surface-

DOI: 10.1021/jp5090795
J. Phys. Chem. C 2015, 119, 2142–2147

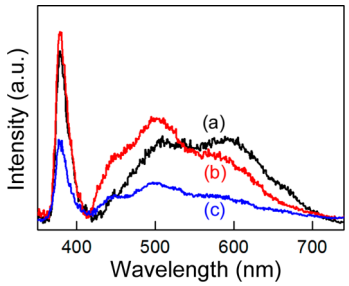

Figure 5. PL (with $\lambda_{excitation}$ = 325 nm) emission spectra of postannealed ZnO:Eu^{3+} nanowalls (a) without and with surface-functionalization of (b) 0.01 M and (c) 0.1 M of enthylenediamine.

functionalization. Evidently, the nanowalls treated with 0.01 M of en in CH_2Cl_2 do not exhibit the sharp feature at 620 nm, in marked contrast to the phen surface-functionalization. The blue-green emission between 450 and 550 nm becomes more intense, as similarly found for the case with the phen treatment at a higher concentration. Together with Figure 4, these results therefore suggest that the emission from Eu^{3+} could be strongly related to the energy-transfer process from a coordinated molecule, such as phen. In addition, the enhancement of the blue and green emissions could be attributed to newly formed defects, such as Zn^{2+}–N complex, on the surface layer of the nanowalls.

These observations suggest that phen adsorbed on the surface of the ZnO:Eu^{3+} nanowalls could play two important roles in the energy transfer mechanism from ZnO (as the energy donor) to Eu^{3+} (as the energy acceptor). Phen is potentially a good acceptor, because its absorption band overlaps well with the band-edge emission band. To account for our observation, we propose a model (shown schematically in Figure 6) for the red emission from Eu^{3+} involving two

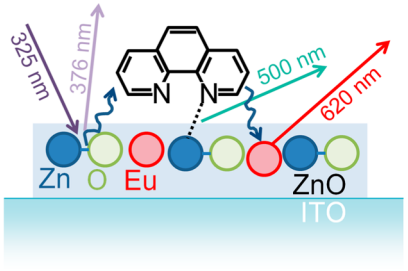

Figure 6. Schematic model for the cascade energy transfer of phen-modified ZnO:Eu^{3+} nanowalls.

consecutive energy-transfer processes, i.e., from ZnO to Eu^{3+} via phen. As shown in Figure 7, the cascade energy transfer begins with excitation of ZnO from the valence band (VB) to upper levels in conduction band, and the subsequent relaxation from upper levels to the lowest level in the conduction band (LCB). Without the surface modification of the ZnO:Eu^{3+} nanowalls by phen, the two possible processes originating from LCB are the radiative decay to VB and the energy transfer to upper levels of the intrinsic defects (such as OH^-, oxygen vacancy V_O, zinc vacancy V_{Zn}, and oxygen interstitials O_i), which result in the band-edge and deep-level emissions, respectively (Figure 7a). When the surface of the nanowalls is treated with phen of a sufficiently low concentration (Figure 7b), a competitive process involving energy transfer from LCB to the excited singlet state of phen also occurs. Furthermore,

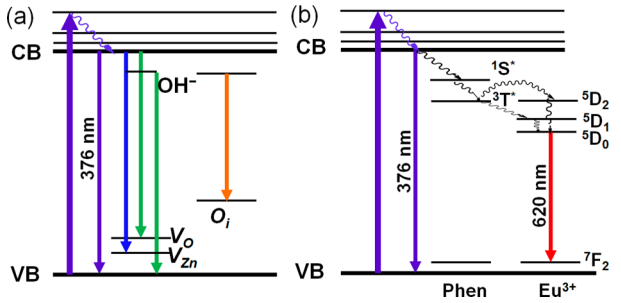

Figure 7. Energy level diagrams for (a) annealed ZnO:Eu^{3+} nanowalls and (b) the cascade energy transfer mechanism in the phen-modified ZnO:Eu^{3+} nanowalls.

following the subsequent intersystem crossing of the singlet excited state ($^1S^*$) to its triplet state ($^3T^*$) in phen, the energy of the excited triplet state of phen is transferred to the near resonant states of Eu^{3+} ($^5D_2$, $^5D_1$), because the energy transfer directly from the singlet state of phen to the Eu^{3+} states is less efficient.

The energy transfer processes from an excited state of a ligand to a rare earth ion in the solid state have been described in the exchange interaction theory by Dexter.[47] In Dexter's model, the energy transfer rate is given by $\exp(-2R)$, where R is the separation between a donor phen and an acceptor Eu^{3+}. When the proximate distance is very close to the Eu-to-N bond distance (2.60 Å), energy transfer from phen to Eu^{3+} could take place very effectively.[45] If the Eu-to-N separation is increased by twice the proximate distance, the energy transfer probability would decrease by more than an order of magnitude. When ZnO:Eu^{3+} nanowalls are treated with a sufficiently low concentration of phen (below 0.050 M, Figure 4c), the phen molecules located within the proximate range of Eu^{3+} ions provide a preferred path in the optical de-excitation process of the nanowalls, and the cascade energy transfer process (from ZnO to phen to Eu^{3+}) would take place efficiently. When the concentration of phen is increased to 0.050 M (Figure 4d), some phen molecules would bind to Zn^{2+} at long distance, which would contribute to additional blue-green emission. However, the overall intensity except the blue-green region is greatly reduced for 0.1 M phen (Figure 4e). Since phen is saturated in the proximate distance range of Eu^{3+}, the additional phen molecules are anticipated to bind to Zn^{2+} and are not able to enhance the probability of cascade energy transfer from ZnO to Eu^{3+}. Furthermore, the additional phen molecules appear to crunch the intensity of the overall spectrum.

■ CONCLUSION

We have successfully embedded Eu into ZnO nanowall structures by using a single-step electrochemical deposition method. Our SEM data show that ZnO nanowalls have become thicker and stacked upon doping with Eu. Our O 1s and Zn 2p XPS results further reveal a ZnO–$Zn(OH)_2$ core–shell structure for the Eu-embedded ZnO nanowalls, similar to that of the pristine ZnO nanowall structure. Eu is found to be uniformly embedded in the ZnO–$Zn(OH)_2$ core–shell nanostructure, as supported by the nearly uniform Eu 3d intensity with increasing Ar^+ sputtering depth. The PL spectral features of the as-grown Eu-embedded ZnO nanowalls are observed to be independent of the Eu^{3+} concentration. Annealing the ZnO:Eu^{3+} nanowall samples yields band-edge emission, while surface modification of the samples by phen

DOI: 10.1021/jp5090795
J. Phys. Chem. C 2015, 119, 2142–2147

generates an additional sharp Eu^{3+} emission at 620 nm. These results show that the energy transfer from ZnO to Eu(III) appears to be extremely weak without phen, and they provide strong support for our proposed cascade energy transfer model. Our findings and the cascade energy transfer model could be extended to provide further insight into rare earth-doped ZnO systems prepared by other embedment process.

EXPERIMENTAL SECTION

Europium-doped ZnO nanowall structures were prepared by electrochemical deposition at 70 °C, described in detail elsewhere.[43,44] Briefly, we employed a potentio/galvanostat electrochemical workstation (CH Instruments 660A) and a three-electrode glass cell, with a Ag/AgCl reference electrode and a Pt wire counter electrode. The working electrode was single-sided polished, SiO_2-passivated float glass coated with an ITO film (200−500 nm thick with a sheet resistance of 4−8 ohm) obtained from Delta Technologies Limited (Minnesota, USA). ZnO nanowall structures were deposited at −1.2 V vs Ag/AgCl by amperometry in a solution of 0.1 M $Zn(NO_3)_2 \cdot 6H_2O$ (Aldrich, ≥99.0% purity) with 0.1 M KCl used as the supporting electrolyte. To prepare Eu-doped ZnO nanowalls, we simply added $Eu(NO_3)_3 \cdot 5H_2O$ (Aldrich, 99.9% purity) solutions of different concentrations (0.01, 0.05, and 0.10 M) to the electrolyte solution and follow the electrochemical deposition procedure. After the deposition, we rinsed the samples with Millipore water thoroughly and dried under nitrogen flow before analysis. Surface modification of Eu-doped ZnO nanowalls were performed by dipping the samples into 1,10-phenanthroline (Aldrich, ≥99% purity) or ethylenediamine (Aldrich, ≥99.5% purity) with various concentrations. For both cases, CH_2Cl_2 (Aldrich, ≥99.9% purity) was used as a solvent.

Scanning electron microscopy (SEM) images were obtained using a field-emission Zeiss UltraPlus microscope. For depth-profiling X-ray photoelectron spectroscopy, we utilized a Thermo-VG Scientific ESCALab 250 Microprobe with a monochromatic Al Kα source (1486.6 eV), and an energy resolution of 0.4−0.5 eV full width at half-maximum. For photoluminescence and excitation spectroscopic measurements, an excitation source of a He−Cd 325 nm laser line and an Oriel 1000 W lamp (operated at 600 W) with an Oriel MS257 monochromator were used, respectively. The spectra were taken by an ARC 0.5 m Czerny-Turner monochromator and a cooled Hamamatsu R-933−14 photomultiplier tube.

ASSOCIATED CONTENT

Supporting Information

PL and excitation spectra of $[Eu(phen)_2] \cdot (NO_3)_3$. This material is available free of charge via the Internet at http://pubs.acs.org.

AUTHOR INFORMATION

Corresponding Author

*(K.T.L.) E-mail: Tong@uwaterloo.ca.

Present Addresses

[§]Department of Chemistry, Yeungnam University, Gyeongsan, Gyeongbuk 712−749, South Korea.

[⊥]Materials Science Center, Indian Institute of Technology, Kharagpur, West Bengal 721 302, India.

Notes

The authors declare no competing financial interest.

ACKNOWLEDGMENTS

This work was supported by the Natural Sciences and Engineering Research Council of Canada.

REFERENCES

(1) Wang, D.; Xing, G.; Gao, M.; Yang, L.; Yang, J.; Wu, T. Defects-Mediated Energy Transfer in Red-Light-Emitting Eu-Doped ZnO Nanowire Arrays. *J. Phys. Chem. C* **2011**, *115*, 22729−22735.

(2) Pal, P. P.; Manam, J. Color Tunable ZnO Nanorods by Eu^{3+} and Tb^{3+} co-doping for Optoelectronic Applications. *Appl. Phys. A: Mater. Sci. Proc.* **2014**, *116*, 213−223.

(3) Li, G.-R.; Dawa, C.-R.; Lu, X.-H.; Yu, X.-L.; Tong, Y.-X. Use of Additives in the Electrodeposition of Nanostructured Eu^{3+}/ZnO Films for Photoluminescent Devices. *Langmuir* **2009**, *25*, 2378−2384.

(4) Ishizumi, A.; Kanemitsu, Y. Structural and Luminescence Properties of Eu-doped ZnO Nanorods Fabricated by a Micro-emulsion Method. *Appl. Phys. Lett.* **2005**, *86*, 253106.

(5) Ohtake, T.; Hijii, S.; Sonoyama, N.; Sakata, T. Electrochemical Luminescence of n-type ZnO Semiconductor Electrodes Doped with Rare Earth Metals under the Anodic Polarization. *Appl. Surf. Sci.* **2006**, *253*, 1753−1757.

(6) Mithal, D.; Kundu, T. Synthesis and Characterization of Gd Doped ZnO Nanocrystals. *Asian J. Chem.* **2013**, *25*, S12−S16.

(7) Al Abdullah, K.; Bakour, B. Semiconductors Elaboration/ZnO Based Varistors for Improving of Stability And Reliability of Electrical Systems Applications by Using the Rare-Earths. *Energy Procedia* **2012**, *19*, 1−14.

(8) Yang, L.; Wang, Z.; Zhang, Z.; Sun, Y.; Gao, M.; Yang, J.; Yan, Y. Surface Effects on the Optical And Photocatalytic Properties of Grapheme-like ZnO:Eu^{3+} Nanosheets. *J. Appl. Phys.* **2013**, *113*, 033514.

(9) Lotey, G. S.; Singh, J.; Verma, N. K. Room Temperature Ferromagnetism in Tb-doped ZnO Dilute Magnetic Semiconducting Nanoparticles. *J. Mater. Sci.: Mater. Electron.* **2013**, *24*, 3611−3616.

(10) Sin, J.-C.; Lam, S.-M.; Lee, K.-T.; Mohamed, A. R. Preparation of Rare Earth-doped ZnO Hierarchical Micro/nanospheres and their Enhanced Photocatalytic Activity under Visible Light Irradiation. *Ceram. Int.* **2014**, *40*, 5431−5440.

(11) Santos, J. G.; Dutra, J. D. L.; Junior, S. A.; Freire, R. O.; Junio, N. B. da C. Theoretical Spectroscopic Study of Europium Tris-(bipyridine) Cryptates. *J. Phys. Chem. A* **2012**, *116*, 4318−4322.

(12) Ma, Y.; Wang, Y. Recent Advances in the Sensitized Luminescence of Organic Europium Complexes. *Coord. Chem. Rev.* **2010**, *254*, 972−990.

(13) Tanner, P. A.; Li, W.; Ning, L. Electronic Spectra and Crystal-Field Analysis of Europium in Hexanitritolanthanate Systems. *Inorg. Chem.* **2012**, *51*, 2997−3006.

(14) Katsuki, D.; Sato, T.; Suzuki, R.; Nanai, Y.; Kimura, S.; Okuno, T. Red Luminescence of Eu^{3+} Doped ZnO Nanoparticles Fabricated by Laser Ablation in Aqueous Solution. *Appl. Phys. A: Mater. Sci. Process.* **2012**, *108*, 321−327.

(15) Zhao, S.; Shu, F.; Li, Y.; Liu, C.; Shan, W.; Cui, Y.; Yang, L. Synthesis and Luminescence Properties of ZnO:Eu^{3+} Nano Crystalline via a Facile Solution Method. *J. Nanosci. Nanotechnol.* **2012**, *12*, 2607−2611.

(16) Terai, Y.; Yoshida, K.; Kamarudin, M. H.; Fujiwara, Y. Photoluminescence Properties of Eu^{3+} Ions in Eu- doped ZnO Grown by Sputtering-Aassisted Metal Organic Chemical Vapor Deposition. *Phys. Status Solidi C* **2011**, *8*, 519−521.

(17) Liu, Y.; Luo, W.; Li, R.; Liu, G.; Antonio, M. R.; Chen, X. Optical Spectroscopy of Eu^{3+} Doped ZnO Nanocrystals. *J. Phys. Chem. C* **2008**, *112*, 686−694.

(18) Ortega, Y.; Fernandez, P.; Piqueras, J. Growth and Cathodoluminescence of Eu Doped ZnO Nanoneedles and Branched Nanoneedle Structures. *J. Nanosci. Nanotechnol.* **2010**, *10*, 502−507.

(19) Wang, M.; Huang, C.; Huang, Z.; Guo, W.; Huang, J.; He, H.; Wang, H.; Cao, Y.; Liub, Q.; Liang, J. Synthesis and Photo-

DOI: 10.1021/jp5090795
J. Phys. Chem. C 2015, 119, 2142−2147

luminescence of Eu-doped ZnO Microrods Prepared by Hydrothermal Method. *Opt. Mater.* **2009**, *31*, 1502−1505.
(20) Yang, Y.; Lai, H.; Tao, C.; Yang, H. Correlation of Luminescent Properties of ZnO and Eu Doped ZnO Nanorods. *J. Mater. Sci: Mater. Electron* **2010**, *21*, 173−178.
(21) Pan, C. J.; Chen, C. W.; Chen, J. Y.; Huang, P. J.; Chi, G. C.; Chang, C. Y.; Rene, F.; Pearton, S. J. Optical and Structural Properties of Eu- diffused and Doped ZnO Nanowires. *Appl. Surf. Sci.* **2009**, *256*, 187−190.
(22) Ebisawa, K.; Okuno, T.; Abe, K. Photoluminescence Properties of Eu^{3+}-Doped ZnO Nanoneedles. *Jpn. J. Appl. Phys.* **2008**, *47*, 7236.
(23) Tanner, P. A.; Yu, L. Photoluminescence of ZnO:Eu^{3+} Nanoflowers. *J. Nanosci. Nanotechnol.* **2008**, *8*, 1307−1311.
(24) Ashtaputre, S. S.; Nojima, A.; Marathe, S. K.; Matsumura, D.; Ohta, T.; Tiwari, R.; Dey, G. K.; Kulkarni, S. K. Investigations of White Light Emitting Europium Doped Zinc Oxide Nanoparticles. *J. Phys. D: Appl. Phys.* **2008**, *41*, 015301.
(25) Ishizumi, A.; Takahashi, Y.; Yamamoto, A.; Kanemitsu, Y. Fabrication and Optical Properties of Eu^{3+}-doped ZnO Nanospheres and Nanorods. *Mater. Sci. Eng., B* **2008**, *146*, 212−215.
(26) Pauporte, T.; Pelle, F.; Viana, B.; Aschehoug, P. Luminescence of Nanostructured Eu^{3+}/ZnO Mixed Films Prepared by Electrodeposition. *J. Phys. Chem. C* **2007**, *111*, 15427−15432.
(27) Joshi, B. N.; Yoon, H.; Kim, H. Y.; Oh, J. H.; Seong, T. Y.; James, S. C.; Yoon, S. S. Effect of Zinc Acetate Concentration on Structural, Optical and Electrical Properties of ZnO Thin Films Deposited by Electrostatic Spray on an ITO Substrate. *J. Electrochem. Soc.* **2012**, *159*, H716−H721.
(28) Singh, T.; Pandya, D. K.; Singh, R. Concentration Dependent Structural and Optical Properties of Electrochemically Grown ZnO Thin Films and Nanostructures. *Appl. Surf. Sci.* **2013**, *270*, 578−583.
(29) Inguanta, R.; Garlisi, C.; Spano, T.; Piazza, S.; Sunseri, C. Growth and Photoelectrochemical Behaviour of Electrodeposited ZnO Thin Films for Solar Cells. *J. Appl. Electrochem.* **2013**, *43*, 199−208.
(30) Kim, Y. J.; Shang, H.; Cao, G. Growth and Characterization of [001] ZnO Nanorod Array on ITO Substrate with Electric Field Assisted Nucleation. *J. Sol-Gel Sci. Technol.* **2006**, *38*, 79−84.
(31) Hsu, C.-L.; Chang, S.-J.; Lin, Y.-R.; Wu, J.-M.; Lin, T.-S.; Tsai, S.-Y.; Chen, I.-C. Indium-diffused ZnO Nanowires Synthesized on ITO-buffered Si Substrate. *Nanotechnology* **2006**, *17*, 516−519.
(32) Lupan, O.; Guerin, V. M.; Tiginyanu, I. M.; Ursaki, V. V.; Chow, L.; Heinrich, H.; Pauporte, T. Well-aligned Arrays of Vertically Oriented ZnO Nanowires Electrodeposited on ITO-coated Glass and Their Integration in Dye Sensitized Solar Cells. *J. Photochem. Photobiol. A: Chem.* **2010**, *211*, 65−73.
(33) Venkatachalam, S.; Hayashi, H.; Ebina, T.; Nakamura, T.; Wakui, Y.; Nanjo, H. Preparation and Characterization of Epitaxial Growth of ZnO Nanotip Arrays by Hydrothermal Method. *J. Colloid Interface Sci.* **2013**, *395*, 64−67.
(34) Wu, H.; Xue, M.; Ou, J.; Wang, F.; Li, W. Effect of Annealing Temperature on Surface Morphology and Work Function of ZnO Nanorod Arrays. *J. Alloy. Compd.* **2013**, *565*, 85−89.
(35) Teng, X.; Fan, H.; Pan, S.; Ye, C.; Li, G. Abnormal Photoluminescence of ZnO Thin Film on ITO Glass. *Mater. Lett.* **2007**, *61*, 201−204.
(36) Ahn, C. H.; Kim, Y. Y.; Kim, D. C.; Mohanta, S. K.; Cho, H. K. A Comparative Analysis of Deep Level Emission in ZnO Layers Deposited by Various Methods. *J. Appl. Phys.* **2009**, *105*, 013502.
(37) Ozgur, U.; Alivov, Ya. I.; Liu, C.; Teke, A.; Reshchikov, M. A.; Dogan, S.; Avrutin, V.; Cho, S.-J.; Morkoc, H. A Comprehensive Review of ZnO Materials and Devices. *J. Appl. Phys.* **2005**, *98*, 041301.
(38) Fan, J.; Güell, F.; Fábrega, C.; Fairbrother, A.; Andreu, T.; López, A. M.; Morante, J. R.; Cabot, A. Visible Photoluminescence Components of Solution-Grown ZnO Nanowires: Influence of the Surface Depletion Layer. *J. Phys. Chem. C* **2012**, *116*, 19496−19502.
(39) Tam, K. H.; Cheung, C. K.; Leung, Y. H.; Djurišić, A. B.; Ling, C. C.; Beling, C. D.; Fung, S.; Kwok, W. M.; Chan, W. K.; Phillips, D. L.; et al. Defects in ZnO Nanorods Prepared by a Hydrothermal Method. *J. Phys. Chem. B* **2006**, *110*, 20865−20871.
(40) Norberg, N. S.; Gamelin, D. R. Influence of Surface Modification on the Luminescence of Colloidal ZnO Nanocrystals. *J. Phys. Chem. B* **2005**, *109*, 20810−20816.
(41) Zhou, H.; Alves, H.; Hofmann, D. M.; Kriegseis, W.; Meyer, B. K.; Kaczmarczyk, G.; Hoffmann, A. Behind the Weak Excitonic Emission of ZnO Quantum Dots: ZnO/$Zn(OH)_2$ Core-Shell Structure. *Appl. Phys. Lett.* **2002**, *80*, 210−212.
(42) Han, M.; Oh, S. J.; Park, J. H.; Park, H. L. X-ray Photoelectron Spectroscopy Study of CaS:Eu and SrS:Eu Phosphors. *J. Appl. Phys.* **1993**, *73*, 4546−4549.
(43) Pradhan, D.; Leung, K. T. Controlled Growth of Two-Dimensional and One-Dimensional ZnO Nanostructures on Indium Tin Oxide Coated Glass by Direct Electrodeposition. *Langmuir* **2008**, *24*, 9707−9716.
(44) Pradhan, D.; Leung, K. T. Vertical Growth of Two-Dimensional Zinc Oxide Nanostructures on ITO-Coated Glass: Effects of Deposition Temperature and Deposition Time. *J. Phys. Chem. C* **2008**, *112*, 1357−1364.
(45) Kang, J.-G.; Kim, T.-J.; Kang, H.-J.; Kang, S. K. Crystal Structures and Luminescence Properties of $[Eu(ODA)\cdot(phen)\cdot 4H_2O]^+$, $[Tb(ODA)\cdot(phen)\cdot 4H_2O]^+$ and $[Tb(ODA)_3]_3^-$ (ODA, oxydiacetate; phen, 1,10-phenanthroline). *J. Photochem. Photobiol. A: Chem.* **2005**, *174*, 28−37.
(46) Lee, J. C.; Choi, K.-S.; Cho, H.-K.; Kang, J.-G. Synthesis and Luminescence of Eu(III) Complexes with Macrocyclic Azacrown Ethers and 1,10-Phenanthroline. *J. Lumin.* **2007**, *127*, 332−338.
(47) Dexter, D. L. A Theory of Sensitized Luminescence in Solids. *J. Chem. Phys.* **1953**, *21*, 836−850.

DOI: 10.1021/jp5090795
J. Phys. Chem. C 2015, 119, 2142−2147